data. Most of the published two-phase heat transfer studies focused on gas-liquid.

Many technical and scientific research efforts have been established in the studies of heat transfer in pipelines. In the last five decades, most published works were reported on heat transfer coefficient correlations and experimental data for forced convection in two-phase gas-liquid in horizontal and vertical pipes. These developed correlations were only applied to some flow regimes within a specific range due to limited available experimental data. Most of the published two-phase heat transfer studies focused on gas-liquid.

Two-phase heat transfer process is dependent on the hydrodynamic behavior of the flows. The flow pattern of oil-water flows is completely different from the gas-oil flows and the distinction is ascribed to the small buoyancy effect and large momentum transfer capacity in the oil-water flows [1]. Also, the research on heat transfer for two-phase oil/water is limited when compared to gas/liquid heat transfer. Some experimental, empirical correlations and theoretical models have been reported for estimating the heat transfer of oil/water flow at different pipeline inclinations [8]. However, no reported CFD model in the open literature has been employed to compute the influence of different flowline inclinations on the HTC for two-phase oil-water flows.

The objective of this paper is to develop a non-isothermal two-phase heat transfer model that is robust enough to span most of the fluid combinations, flow patterns, flowline orientations, and flow rates. The developed heat transfer model is validated with the experimental results for various flow patterns and HTC of oil-water two-phase flow in inclined and horizontal pipes. To this end, HTC and flow patterns for two-phase oil-water flows at downward flowline inclinations are also examined.
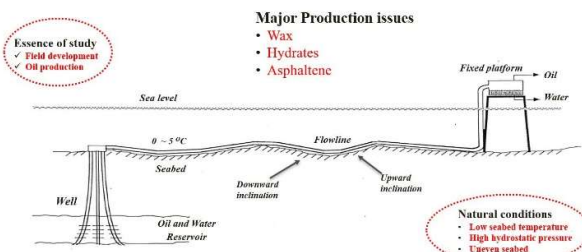

Figure 1. Schematic representation of oil-water two-phase subsea production

Mathematical Model

Several studies on the hydrodynamics and thermal modeling of different flow behavior and flowline orientations are performed, centering on computing the HTC, velocity and temperature distribution, pressure drop, and flow patterns.

Governing Equations A 3D non-isothermal two-phase Newtonian flow model has been developed in this section. The governing equations comprise mass conservation, momentum conservation, and energy conservation equation. From the preceding analysis, the mathematical models of non-isothermal two-phase Newtonian flow are expressed below:

Mass conservation equation. At the flowline cross-section in the axial direction, the total mass of the oil-water phases is constant. The conservation equation is shown as follows.

$$\frac{\partial \rho}{\partial t} + \nabla.(\rho U) = 0 \qquad (1)$$

where ρ and U are the density of the velocity of the two-phase fluid.

Momentum conservation equation. Assuming an incompressible two-phase fluid flow, the Navier-Stokes and the Volume of Fluid equations of a fully developed flow are expressed as:

$$\frac{\partial \rho U}{\partial t} + \nabla.(\rho UU) = \nabla P + \nabla.\left[\mu_{eff}(\nabla U + \nabla U^T)\right] + (\rho g \sin\theta) + F_s \qquad (2)$$

$$\frac{\partial \alpha}{\partial t} + \nabla.(\alpha U) + \nabla.(1-\alpha)\alpha U_r) = 0 \qquad (3)$$

where U is the velocity in the axial direction, ∇P is the pressure gradients in the stream's direction, g is the acceleration due to gravity, θ is the inclination angle, μ_{eff} is the effective dynamic viscosity which is the summation of the molecular and turbulent viscosity ($\mu + \mu_t$), U_r is the relative velocity between phases, α is the fluid volume fraction, and F_s is the body force in the axial direction.

Turbulence model. Because of the characteristics of turbulence in two-phase fluid flow, the turbulent fluctuation imposes additional momentum and energy transfer. Therefore, turbulent models are deployed to simulate momentum and energy transfer phenomena. The LRN *k-ε* model is introduced to account for the near-wall treatment by the addition of damping functions into the turbulent viscosity. The turbulent kinetic energy and dissipation are defined by:

$$\frac{\partial (\rho k)}{\partial t} + \nabla.(\rho k U_i) = \frac{\partial}{\partial x_j}\left[\Gamma_k\left(\frac{\partial k}{\partial x}\right)\right] + G_k + G_b - \rho\varepsilon - Y_m + S_k \qquad (4)$$

$$\frac{\partial (\rho\tilde{\varepsilon})}{\partial t} + \nabla.(\rho\tilde{\varepsilon}U_i) = \frac{\partial}{\partial x_j}\left[\Gamma_\varepsilon\left(\frac{\partial\varepsilon}{\partial x_j}\right)\right] + C_1 f_1 \frac{\varepsilon}{k}(G_k + G_b) - C_2 f_2 \rho\frac{\varepsilon^2}{k} + E + D + S_\varepsilon \qquad (5)$$

where G_k and G_b are the productions of turbulence kinetic energy, Y_m is the fluctuation dilation incompressible turbulence, and turbulent viscosity is $\mu_t = \frac{f_\mu\, C_\mu\, \rho k^2}{\varepsilon}$, $\Gamma_k = \left(\mu + \frac{\mu_t}{\sigma k}\right)$, $\Gamma_\varepsilon = \left(\mu + \frac{\mu_t}{\sigma\varepsilon}\right)$. For the k-ε model, $C_\mu = 0.09$, $C_1 = 1,92$, and $C_2 = 1.3$ are the model constants. f_μ, f_1, and f_2 are the functions specially employed for the near-wall treatment. E and D are additional terms to further stabilize dissipation and diffusion in the area of the walls, S_k and S_ε are the source terms.

Energy conservation equation. The heat-transfer process especially with the turbulent flow is valuable for both engineering and due to its occurrence in numerous industrial applications.

Thus, the energy equation is added to the governing equations. Assuming a quasi-transient state in which axial heat conductive heat effect is neglected, no added source term in the energy equation. The energy equation is shown as:

$$\frac{\partial T}{\partial t} + \nabla_z \cdot \left(\rho C_p U T\right) = \nabla_x \cdot \left[\frac{\mu_a C_p}{Pr}(\nabla_x T)\right] +$$

$$\nabla_y \cdot \left[\frac{\mu_a c_p}{Pr}(\nabla_y T)\right] \quad\quad (8) \text{ where}$$

T is the temperature of the two-phase fluid, C_p is the specific heat capacity of the two-phase fluid, $Pr = C_p \frac{\mu_a}{\lambda}$ is the Prandtl number, and λ is the thermal conductivity of the two-phase fluid.

Boundary Conditions The simulation of two-phase oil-water flow is considered axisymmetric. At the onset of the simulation (time = 0), an equal volume fraction of oil-water was infused at the inlet domain of the pipe with different superficial inlet velocities, the outlet permits the mixed flowing fluids to come out of the domain with a pressure of zero, while the no-slip condition for velocity was assumed at the pipe wall. A uniform wall heat flux value ranging from 15,100 - 24,800 W/m² and at atmospheric pressure (room temperature of about 25°C) were used. Since the flow problem was deemed axisymmetric, the computational domain was specified as half-pipe, and the symmetry-plane boundary condition was used in the longitudinal pipe section (X-Z plane in Fig. 2). In summary, the appropriate boundary conditions are utilized according to Table 1.

Table 1. Boundary Conditions.

Variables	Inlet	Outlet	Wall
U	$U_{w,o} = U_{w,\&o,inlet}$	$\frac{\partial U_{w,o}}{\partial x} = 0$	$U_{w,\&o,wall} = 0$
T	$T_{w,o} = T_{inlet}$	$\frac{\partial T}{\partial x} = 0$	$h = (T_{wall} - T_m) = \lambda \frac{\partial T}{\partial r}$
P-pgh	$\frac{\partial P}{\partial x} = 0$	$P_{w\&o,outlet} = 0$	$\frac{\partial P}{\partial z} = 0$
k	$k_{w,o} = k_{w,\&o,inlet}$	$\frac{\partial k_{w,o}}{\partial x} = 0$	$k_{w,o,g} = k_{wall}$
μ_t	$\mu_{t,cal} = 0$	$\mu_{t,cal} = 0$	$\mu_{t,kwallfunc} = \mu_{t,wall}$
ε	$\varepsilon_{w,o} = \varepsilon_{inlet}$	$\frac{\partial \varepsilon_{w,o}}{\partial x} = 0$	$\varepsilon_{wallfunc} = \varepsilon_{wall}$

Numerical Method

OpenFOAM v.5.0 was used to simulate different two-phase flow cases. The two-phase flow is calculated by using the developed solver based on the Volume of Fluid approach. Turbulence effects and their influence on the flow were performed for all simulations using RANS models. Discretization of the transport equation is executed using the Finite Volume Method. The Euler scheme is used for temporal and time discretization and spatial discretization is a standard second-order scheme.

Model Geometry and Mesh The 3D flowline geometry was constructed with a diameter and length of 0.011m and 1.8 m respectively. The mesh consisting of structured hexahedral cells is bounded by three types of boundary faces (inlet, outlet, and wall), as seen with the 3D flowlines in Fig.1. Both geometry and the structured mesh were created by the blockMesh utility in OpenFOAM.
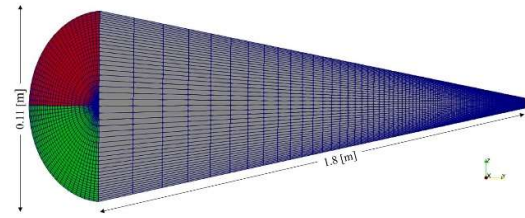

Figure 2. Computational half-pipe domain for the axisymmetric two-phase oil-water flow.

Models Validation

Prediction of Flow Patterns at different Flowline Inclinations The proposed model is validated by the experimental investigation of [8]. Boostani et al. studied the heat transfer coefficient of oil-water flow in horizontal and inclined pipes. The superficial Reynolds number of the water-phase, Re_{sw} was maintained at 6772, while the superficial Reynolds numbers of the oil-phase Re_{so} varied at intervals. To validate the studied results, the numerical results of flow patterns and HTCs for oil-water two-phase flow at different flowline inclinations are compared with experimental data. Therefore, the thermohydraulic calculations are both tested and established.

The oil-water flow pattern maps for different flowline orientations are classified in line with the definitions of [8] and [1]. The observed flow patterns are stratified flow (ST), stratified flow with a mixed interface (ST & MI), plugs of oil in water (Po/w), plugs of water in oil (Pw/o), dispersion of water in oil & oil in water (Dw/o & o/w), and dispersion of oil in water (Dw/o) flows.

Table 2 illustrates a comparison between numerical and measured flow patterns visualized at different Re_{so} (≈ 450 – 3750) and Re_{sw} kept at 6772. The 3D non-isothermal two-phase flow model predicted the observed flow patterns of oil-water flow very reliably. For instance, in horizontal flow, the performance of the model was remarkably good for predicting Po/w, ST & MI, Dw/o & o/w, and Dw/o flows. Also, for flowline inclinations of -10°, -4°, and +10°, the flow patterns visualized using the proposed model are mostly ST & MI, with Po/w, Dw/o & o/w, and Dw/o only observed at low and very high Re_{so}. Varying the inclination angles downward reduces the gravitational forces, which are most pronounced at upward inclinations, and tends to decelerate the denser water phase in the upward direction. Water is the fastest-moving phase during the downward flow and it reduces the hold-up.

Effect of flowline inclinations and Flow pattern on HTC Figure 2 describes the comparison between the numerical and measured HTC values under various Re_{so} of about 450 – 3750 when the Re_{sw} is 6772 at different flow inclinations (0°, +4°). The numerical HTC results are slightly different from the experimental values as the flow patterns changes from Po/w to Dw/o. The relative errors

between the calculated HTC and experimental results at Re_{so} of approximately 450 are 3% for the 3D model, where there is a decrease of HTC due to the flow pattern change from Po/w to ST & MI. At a Re_{so} of about 1280, the relative error for the horizontal flow where the HTC value is higher than the inclined flow is 2% for the 3D model. In summary, the results of the relative errors obtained from the developed model and Boostani's values are within 3%, which demonstrates the model's accuracy. Furthermore, the numerical HTC results at flowline inclinations of -10°, -4°, and +10° are shown in Fig. 3. In downward flows, the flow pattern change from Po/w to ST & MI regime causes a decrease in HTC values. Further increase in the oil flow rates coupled with gravity forces working in the reverse direction to the upward inclination flow enhances the interfacial mixing of the oil-water flow, resulting in HTC increase for ST & MI to Dw/o & o/w flow transition. Changing the flowline inclination from a horizontal to a downward flow regime increases the HTC in the flow transition. However, the HTC for horizontal flow is higher than the downward/upward flows at Re_{so} values of about 1200-1800. This difference is traceable to the flow pattern observed at these Re_{so} values and the difference in turbulence forces. In conclusion, the proposed model was able to compute the HTC results for two-phase oil-water flows and it is a function of the flow patterns.

Table 2. Flow pattern comparison of present work with experimental data.

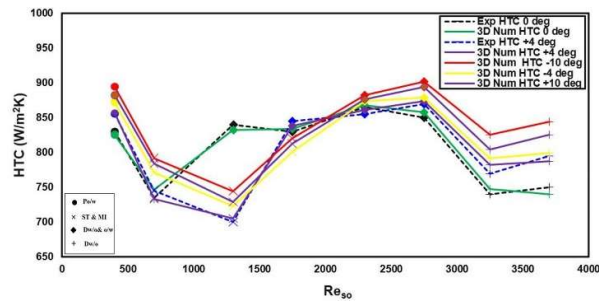| Flowline inclinations						
0°		+4°		-10°	-4°	+10°
Exp	3D Predict	Exp	3D Predict	3D Predict	3D Predict	3D Predict
Po/w	Po/w	Po/w	Po/w	Po/w	Po/w	Po/w
ST&MI	ST&MI	ST&MI	ST&MI	ST&MI	ST&MI	ST&MI
Dw/o& o/w	Dw/o& o/w	ST&MI	ST&MI	ST&MI	ST&MI	ST&MI
Dw/o& o/w	Dw/o& o/w	Dw/o& o/w	Dw/o& o/w	ST&MI	ST&MI	ST&MI
Dw/o& o/w	Dw/o& o/w	Dw/o& o/w	Dw/o& o/w	Dw/o& o/w	Dw/o& o/w	Dw/o& o/w
Dw/o& o/w	Dw/o& o/w	Dw/o& o/w	Dw/o& o/w	Dw/o& o/w	Dw/o& o/w	Dw/o& o/w
Dw/o	Dw/o	Dw/o	Dw/o	Dw/o	Dw/o	Dw/o
Dw/o	Dw/o	Dw/o	Dw/o	Dw/o	Dw/o	Dw/o

Figure 3. The HTC variation at different 3D flowline inclinations as a function of Re_{so}.

Results and Discussion

The developed numerical model is first implemented to generate validated numerical results of flow patterns and HTC for oil-water two-phase flow at different flowline inclinations. Thereafter, the prediction of the hydrodynamic and thermal behavior of the two-phase flow is described

Liquid holdup, HL The average HL at the flowline cross-section is expressed in Fig. 4 for flow having Re_{so} values of about 450 – 2750 and Re_{sw} = 6772. Po/w is observed at Re_{so} of 450 with a higher water HL than oil and in the continuous water phase, SI & MI is noticed as Re_{so} increases above 450 showing almost equal HL of oil and water in the continuous. oil-water phases. At Re_{so} lower than 2750, Dw/o & o/w flow regime is observed that the HL of water decreases during the transition, which indicated that the dispersed water continuous flow moved much faster than the dispersed oil continuous phase. Additional increase in Re_{so} to ≈2750 results in Dw/o where HL of water further reduces, which demonstrated that the dispersed water droplets moved faster than the continuous oil phase. it can be seen that the water droplet concentration increased towards the flowline midpoint where the velocity is highest. Lift forces were responsible for the increased droplet concentration at the midpoint.
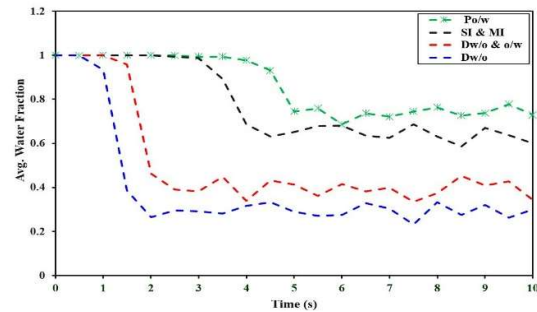

Figure 4. The liquid fraction in the flowline length of 0.9m

Pressure along flowline length The value of the pressure gradient along the flowline length was investigated at different Re_{so} values (450 – 2750) while maintaining Re_{sw} = 6772 as shown in Fig. 5. It is observed in horizontal flow that the frictional pressure gradient increases in the transition from Po/w to Dw/o flow due to increased turbulence forces. Based on Po/w, when the inlet oil flow rate increases, the oil-water flow pattern transition to ST & MI. The pressure variation rose as the water continuous phase in Po/w was replaced with an oil-water continuous phase, which increases the wall friction and frictional pressure drop. Increasing the oil flow rates, the oil-water flow changes to Dw/o & o/w flow regime, and the pressure variation increases because of the high inlet velocity and the amount of continuous oil-water phases in the flowline. Based upon Dw/o & o/w, a further increase in the inlet oil flow rates, the oil-water flow changes to Dw/o. The pressure gradient further increases as the continuous oi-water phases are substituted with an oil continuous phase, which increases the frictional pressure drop. However, due to the influence of the hilly-terrain flowline as seen in this study. The frictional pressure gradients at the different flow transitions from Po/w to Dw/o are in general noticed to be lower than horizontal flow. This was ascribed to a higher in-situ water fraction or holdup in the upward and reduced

holdup in the downward flows. In essence, confirms the investigations that flow pattern has a big impact on the measured pressure gradient.

Temperature variations The temperature distribution at the midpoint of the flowline cross-section for different inclinations is shown in Fig. 6. As can be seen, the temperature of both oil and water phases increases because of the higher surrounding temperature through the constant wall heat flux and the convective heat transfer effects. As the oil superficial velocity increases at constant water superficial velocity during a transition from Po/w to Dw/o, the temperature of oil and water keeps increasing from the horizontal flowline wall to the fluid interface, and the temperature gradient in the radial direction of the water phase is smaller than that of the oil phase gradient. This is because oil has a lower specific heat transfer heat capacity ($c_{p)}$) than water and the phenomenon entails heat being transferred from the wall to the oil interface faster.
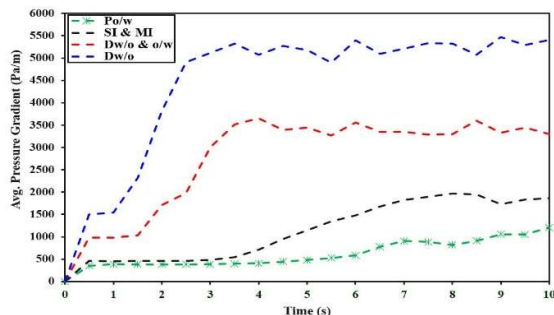

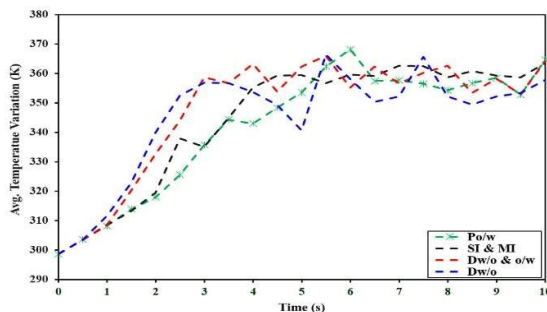Figure 5. Pressure gradient at the flowline length of 1.8m

Figure 6. Temperature variation at flowline length of 0.9m

Conclusions

A non-isothermal two-phase oil-water flow model for different flowline orientations and flow patterns is developed. LRN k-ε is deployed to simulate the turbulence viscosity based on the solution of the momentum conservation and energy conservation equations. The computed results were validated with experimental data in the literature with a relative error of 3%, which demonstrates the high accuracy of the model. Afterward, a study of non-isothermal oil-water simulations at different flow patterns and flowline inclinations is carried out. The flow patterns, HTC along the flowline at different

flow rates, Newtonian behavior, and flowline orientations are predicted. Detailed flow information like liquid holdup, pressure gradient, and temperature on flowline cross-section at different flowline orientations and flow patterns are investigated. The main conclusions of this work obtained are:

- In the horizontal flowline, the in-situ water volume fraction decreases as the oil superficial velocity increases at constant water superficial velocity during a transition from Po/w to Dw/o. For upward flow, the in-situ water volume fraction increases because the denser phase decelerates due to gravity forces. Conversely, a decreased holdup in the downward flow results from a velocity increase of the denser phase.
- The frictional pressure gradient in the horizontal flowline increases through the transition from Po/w to Dw/o flow. The pressure drops rose as the water continuous phase was replaced with an oil continuous phase, which increases the wall friction. The frictional pressure gradients in upward and downward flows decrease due to a higher in-situ water fraction or holdup.
- The average temperature of the two-phase oil-water horizontal flowline increases from the wall to the fluid interface, and the temperature gradient in the radial direction of the water phase is smaller than that of the oil phase gradient. In upward flow, the temperature is higher than that of horizontal flow due to a higher liquid holdup by gravitational forces in the upward flow.

In the end, the developed numerical model could be generally employed to compute fluid properties and other operating variables in the two-phase flowlines transportation system.

Acknowledgments

Responsibility Notice

The authors are responsible for the paper content.

References

[1] Oddie G, Shi H, Durlofsky LJ, Aziz K, Pfeffer B, Holmes JA. Experimental study of two and three-phase flow in large diameter inclined pipes. International Journal of Multiphase Flow 2003;29:527–58.
[2] Sunday N, Settar A, Chetehouna K, Gascoin N. Numerical Study of the Behavior of Two-Phase Hydrocarbon Flow Phenomena in Horizontal Flowlines using OpenFOAM. Chemical Engineering & Technology 2022.
[3] Sunday N, Settar A, Chetehouna K, Gascoin N. Numerical modeling and parametric sensitivity analysis of heat transfer and two-phase oil and water flow characteristics in horizontal and inclined flowlines using OpenFOAM. Petroleum Science 2022.

[4] Sunday N, Settar A, Chetehouna K, Gascoin N. Numerical Heat Transfer Analysis of Two-Phase Flow in Horizontal and Inclined Flowline using OpenFOAM. ICHMT DIGITAL LIBRARY ONLINE, Begel House Inc.; 2022.

[5] Sunday N, Settar A, Chetehouna K, Gascoin N. An Overview of Flow Assurance Heat Management Systems in Subsea Flowlines. Energies 2021;14:458.

[6] Amundsen L. An experimental study of oil-water flow in horizontal and inclined pipes (Ph.D. Thesis). Norwegian University of Science and Technology 2011.

[7] Sunday N, Settar A, Chetehouna K, Gascoin N. Numerical study and sensitivity analysis of two-phase oil-water flow and heat transfer in different flowline orientations using OpenFOAM. Case Studies in Thermal Engineering 2022;40:102465.

[8] Boostani M, Karimi H, Azizi S. Heat transfer to oil-water flow in horizontal and inclined pipes: Experimental investigation and ANN modeling. International Journal of Thermal Sciences 2017;111:340–50.